PHILOSOPHICAL MAGAZINE B, 2000, VOL. 80, NO. 10, 1857–1868

Short-range order and luminescence in amorphous silicon oxynitride

V. A. GRITSENKO†

Institute of Semiconductor Physics, 630090, Lavrentiev Avenue 13, Novosibirsk, Russia

YU. G. SHAVALGIN, P. A. PUNDUR

Institute of Solid State Physics, University of Latvia, 8 Kengaraga Street, Riga LV 1063, Latvia

HEI WONG

Department of Electronic Engineering, City University, Tat Chee Avenue, Kowloon, Hong Kong, China

and W. M. KWOK

Chemistry Department, The Chinese University of Hong Kong, Hong Kong, China

[*Received 13 August 1999 and accepted 17 June 2000*]

ABSTRACT

Using Si 2p core-level X-ray photoelectron spectroscopy, we found that the short-range order in amorphous silicon oxynitride (a-SiO_xN_y) can be quantitatively described by a random bonding model. Results also show that the second and even further neighbours of the Si in the network affect the chemical shifts of the X-ray photoelectron spectra. Cathodoluminescence and photoluminescence of a-SiO_xN_y with different compositions are also measured. A red band with energies of 1.8–1.9 eV, a blue band with an energy of 2.7 eV and ultraviolet bands with energies of 13.1, 3.4–3.6, 4.4–4.7 and 5.4 eV were observed. The 1.8–1.9 eV band is attributed to the O and N atoms with an unpaired electron and the 2.7 eV band is attributed to the twofold-coordinated Si atom with two electrons (sililene centre). The ultraviolet bands are assumed to be related in the Si—Si bonds.

§1. INTRODUCTION

It is suggested that the conventional thermal oxide used as the gate insulator in metal–oxide–semiconductor (MOS) devices will be replaced by amorphous silicon

† Present address: Department of Electronic Engineering and Department of Chemistry, The Chinese University of Hong Kong, Shatin, New Territories, Hong Kong. PR China. Email: vladimir@ee.cuhk.edu.hk or grits@isp.nsc.ru.

Philosophical Magazine B ISSN 1364–2812 print/ISSN 1463–6417 online
http://www.tandf.co.uk /journals

oxynitride (a-SiO_xN_y) in future nanoscale structures for several reasons. The Si—Si bonds (hole traps) at the Si–oxide interface can be reduced greatly with nitridation. In addition, B penetration from the p-type polycrystalline Si gate can also be blocked effectively by using oxynitride (Lu *et al.* 1996). However, the defect density in the oxynitride is still high and is the major constraint for electronic properties of the gate oxynitride in MOS devices. To obtain a better insight into the gate oxynitride properties it is essential to study the short-range order and defect properties. However, investigation of the defect origins in nitrided oxide is very difficult because of the non-uniform composition. For ease of study, we use bulk oxynitride films prepared by the low-pressure chemical vapour deposition (LPCVD) technique. Although the electrical properties of nitrided oxide and LPCVD oxynitride may not be the same, there are some similarities in the defect origins at the interface. It was found that the structural defects due to short-range order in a-SiO_xN_y can be electrically active and result in the device characteristic degradation. With this connection, this work aims to study the short-range order by X-ray photolectron spectroscopy (XPS). We found that the short-range order and defect properties in the oxynitride films can be explained with the random-bonding (RB) model. To validate the RB model, both photoluminescence (PL) and cathodoluminescence (CL) measurements are conducted to study the radiative defect properties.

a-SiO_xN_y consists of Si—N and Si—O bonds. The chemical bonding in a-SiO_xN_y is governed by the octet $8-n$ Mott rule (Gritsenko *et al.* 1998b). According to this rule, each Si atom is coordinated by four O and/or N atoms, each O atom (as in SiO_2) is coordinated by two Si atoms and each N atom (as in Si_3N_4) is threefold coordinated by Si atoms. The Si—O and Si—N bonds create five sorts of tetrahedron: a-$SiO_\nu N_{4-\nu}$, where $\nu = 0$, 1, 2, 3 and 4. However, the Mott rule does not tell us the distribution of Si—N and Si—O bonds in the oxynitride. The chemical bond distribution in a bulk material is described by short-range order. For binary amorphous tetrahedral alloys, two extreme models for the short-range order are developed which are the random-mixture (RM) model and the RB model (Philipp 1972, Raider *et al.* 1976, Gritsenko *et al.* 1981, Kubler *et al.* 1983, Karcher *et al.* 1984, Britov *et al.* 1985, Hasegawa *et al.* 1992). These models have been widely used to describe the structure of two key dielectrics in semiconductor devices: non-stoichiometric or almost stoichiometric amorphous silicon oxide (a-SiO_x) with $0 < x \leqslant 2$ and amorphous silicon nitride (a-SiN_x) with $0 < x \leqslant 4/3$. According to the RM model, a-SiO_x is composed of a-SiO_2 and a-Si phases, and a SiN_x consists of a-Si_3N_4 and a-Si phases. With this scenario, a-SiO_x consists of SiO_4 and $SiSi_4$ tetrahedra only whereas a-SiN_x consists of SiN_4 and $SiSi_4$ tetrahedra only. If we assume that the structure of a-SiO_xN_y is described by the RM model, then it should be a mixture of SiO_2 and Si_3N_4, whereas the RB model suggests that the a-SiO_x and a-SiN_x consists of $SiO_\nu Si_{4-\nu}$ and $SiN_\nu Si_{4-\nu}$ ($\nu = 0$, 1, 2, 3 and 4) tetrahedra respectively (Gritsenko *et al.* 1981, Kubler *et al.* 1983).

The experimental details are given in next section. In § 2, XPS results are presented and the RB model for describing the short-range order in the oxynitride is given. The CL and PL studies on the oxynitride films are presented in § 3 and § 4 respectively. Defect types are identified on the basis of their energy levels. As will be seen later, these results support the RB model presented in § 2. Finally, in § 6, further remarks on the short-range order and defect properties of the oxynitride are presented.

§ 2. Samples and experiment

a-SiO_xN_y films of different compositions were prepared on Si⟨100⟩ substrates by LPCVD from SiH_4, NH_3 and O_2 source at 875°C. We used XPS to determine the a-SiO_xN_y composition and infrared spectroscopy to detect the concentration of hydrogen bonds. For infrared measurements, samples with an oxynitride thickness of about 1000 Å were used. Samples with an a-SiO_xN_y thickness of about 200 Å were used for XPS measurements to reduce the charging effect. The samples were first etched in 1 : 30 HF : methanol solution for 2 min to remove native oxide and then rinsed by methanol. For binding energy reference, the samples were dipped into cyclohexane followed by a N_2 blow-dry before being put into the XPS system. All the binding energies were referenced to the C 1s peak of cyclohexane at 285.0 eV. Charge neutralizer was used for the measurements when serious positive charging appeared. The composition of a-SiO_xN_y was determined with XPS using thermal SiO_2 and nearly stoichiometric LPCVD silicon nitride (Si_3N_4) as the 'standard', which was produced from mixture of SiC_4 and NH_3 at 800°C with the ratio $SiC_4 : NH_3 = 1 : 10$. In these 'standard' Si_3N_4 samples, absorption at 3330 cm^{-1}, which is attributed to the Si_2N—H stretch vibration, was observed. The density of Si_2NH was found to be 2.1×10^{21} cm^{-3}. The calculated chemical composition of the 'standard' sample was $SiN_{1.41} : H_{0.05}$. For XPS measurements, the samples were dipped into a solution of 1 : 30 HF : deionized water to remove the surface oxide. Infrared absorption spectra were measured with a single-beam Nicolett Magna-IR 555 spectrometer with a resolution of 4 cm^{-1}.

The CL spectra were measured at room temperature in vacuum (10^{-6} Torr). The electron-beam energy was kept at 5 keV and the current was 3×10^{-6} A. The exited square was about 0.5 mm^2. Two cooled photomultipliers were used to detect CL in the ranges 220–500 and 620–720 nm. CL spectra were normalized to the sensitivity of the recorded system. PL measurements were measured at room temperature with the excitation by a H lamp (DDS-400), using a grating monochromator (MDR-2).

§ 3. X-ray photoelectron spectroscopy results and random-bonding model

Figure 1 shows the X-ray photoelectron spectra of Si 2p core levels of a-SiO_xN_y films of different compositions. Only one peak is found for different samples. This observation cannot be explained with the RM model. According to the RM model, an X-ray photoelectron Si 2p spectrum should have two components, corresponding to the a-SiO_2 and a-Si_3N_4 phases respectively. To obtain a deeper insight, we compare the experimental Si 2p spectra with spectra simulated using both the RB and the RM models. According to the RB model, a-SiO_xN_y is composed of five types of tetrahedron described by $SiO_\nu N_{4-\nu}$ (where $\nu = 0$, 1, 2, 3 and 4). To make a theoretical calculation, we need to know the peak positions and widths of the distribution function for the five tetrahedra. The distribution function of the $SiO_\nu N_{4-\nu}$ tetrahedra in a-SiO_xN_y in the RB model is described by

$$W(\nu,x,y) = \left(\frac{2x}{2x+3y}\right)^{\nu}\left(\frac{3y}{2x+3y}\right)^{4-\nu}\frac{4!}{\nu!(4-\nu)!}. \tag{1}$$

Equation (1) assumes that a-SiO_xN_y does not contain any intrinsic defects, such as ≡Si—Si≡, =N—N=, ≡Si—O—O—Si≡ and =N—O— bonds. Equation (1) can be used to describe quantitatively the relative probability of the five sorts of

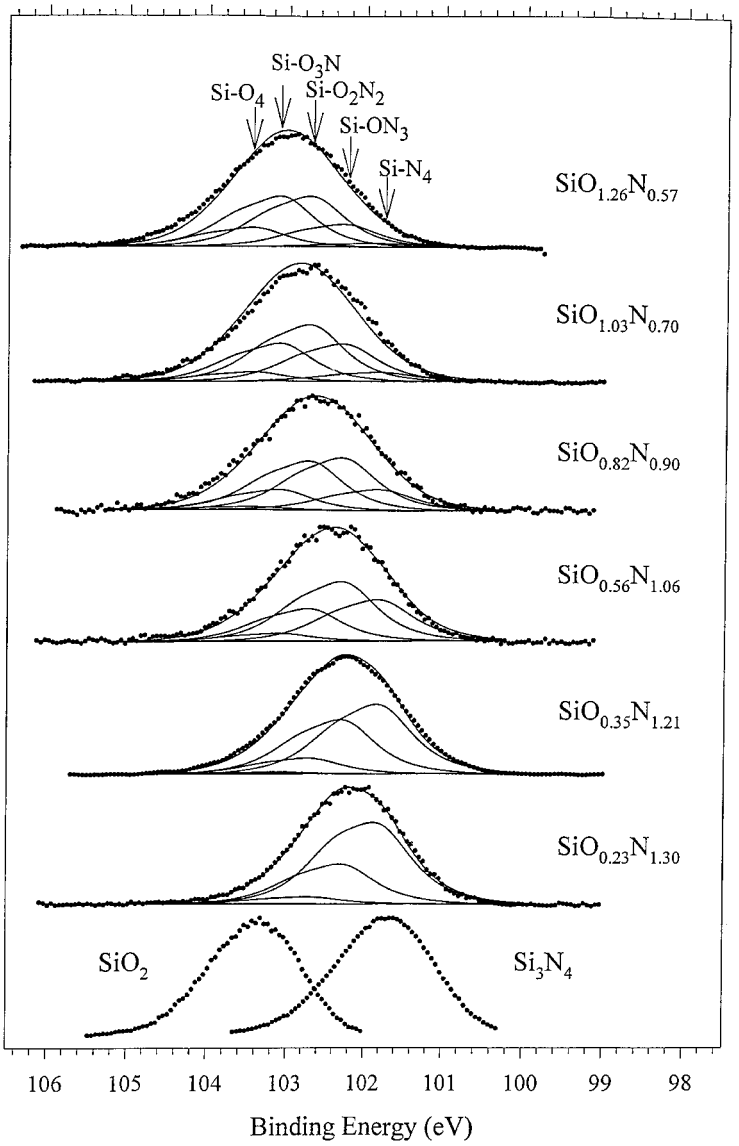

Figure 1. X-ray photoelectron Si 2p spectra of a-SiO_xN_y with different compositions: (●) experimental spectra; (——), simulated spectra.

$SiO_\nu N_{4-\nu}$ tetrahedra in a-SiO_xN_y. To determine the chemical shift of the Si 2p peaks for the tetrahedra SiO_4, SiO_3N, SiO_2N_2, $SiON_3$ and SiN_4 in a-SiO_xN_y, we extended the Hasegawa *et al.* (1992) model for binary alloys of a-SiO_x and a-SiN_x to ternary alloys. For a tetrahedron of $SiO_\nu N_{4-\nu}$ with a bonding unit $Si_kO_mN_n$, the partial charge $P_j(\nu)$ of atom j can be determined by

$$P_j(\nu) = \frac{S_{SiON} - S_j}{2.086 S_j^{1/2}} \tag{2}$$

Table 1. Calculated partial charges on Si, O and N atoms of the five tetrahedra in a-SiO_xN_y.

ν	Tetrahedron	Bonding unit	S_{SiON}	$P_{Si}(\nu)$	$P_O(\nu)$	$P_N(\nu)$
0	SiN_4	Si_3N_4	3.69	0.242	—	−0.182
1	$SiON_3$	Si_2ON_2	3.85	0.288	−0.286	−0.145
2	SiO_2N_2	$Si_3O_2N_2$	4.00	0.330	−0.255	−0.112
3	SiO_3N	$Si_6O_9N_2$	4.13	0.369	−0.227	−0.081
4	SiO_4	SiO_2	4.26	0.404	−0.201	—

where j = Si or N, and $S_{SiON} = (S_{si}^k S_O^m S_N^n)^{1/(k+m+n)}$ is the Sanderson electronegativity of Si in the bonding unit of $Si_kO_mN_n$ (table 1). Here $S_{si} = 2.84$, $S_O = 5.21$ and $S_N = 4.49$ are the Sanderson electronegativities of Si, O and N atoms respectively (Pauling 1960). The bonding units corresponding to the five tetrahedra and the calculated partial charges are given in table 1 where the Sanderson electronegativity S_{SiON} for different bonding units is also shown.

Using the Si $2p_{3/2}$ positions of a-SiO_2 and a-Si_3N_4, we determined the Si $2p_{3/2}$ positions of the remaining three tetrahedra, namely $SiON_3$, SiO_2N_2 and SiO_3N. We used the XPSPEAK 3.1 program to simulate the Si 2p peaks based on the RB model. Simulation was made with Si $2p_{1/2}$-Si $2p_{3/2}$ spin doublet splitting at 0.61 eV. The same values of the full width at half-maximum (FWHM) for Si $2p_{3/2}$ and Si $2p_{3/2}$ peaks for each component were used. For all the six measured a-SiO_xN_y samples, the same values of chemical shifts and FWHMs of the five tetrahedra were used for simulating the Si 2p spectra.

As shown in figure 1, it is found that the experimental Si 2p spectra of a-SiO_xN_y can be quantitatively fitted with the RB model. It suggests that the short-range order in a-SiO_xN_y can be quantitatively described by the RB model. In figure 1, short-range order in Si-rich a-SiO_x which is approximated with RM model (Gritsenko *et al.* 1981, Gritsenko 1993) is also shown for comparison. Figure 1 further shows that the Si 2p peak maximum shifts towards higher binding energies with increase in the O content in a-SiO_xN_y. This effect was also observed previously (Raider *et al.* 1976, Britov *et al.* 1985). This observation can be explained as follows. Since each Si 2p peak consists of five components corresponding to the five different tetrahedra and since the electronegativity of O is larger than that of N, an increase in the O content leads to more $SiO_\nu N_{4-\nu}$ tetrahedra with high values of ν and causes more positive charges accumulated on Si.

Figure 2 depicts the chemical shifts of Si 2p, N 1s and O 1 in a-SiO_xN_y. These chemical shifts qualitatively support the RB model. As shown in figure 2, the binding energies of the Si 2p, N 1s and O 1s levels increase with increase in the O content. According to the additive effect, the charge transfer per Si—O bond and Si—N bond should be constant, which is independent of the types of atom other than the nearest neighbour (Pasquarello *et al.* 1995, Zhang *et al.* 1998). That is the binding energies of the N 1s and O 1s levels should be constant and do not depend on the chemical composition of a-SiO_xN_y. Hence, the additive model does not agree with the experimental observation. The chemical shifts of the O 1s and N 1s levels can be explained by the decrease in the effective negative charge on N and O atoms, which is related to the induction effect. Chemical shifts of the O 1s and N 1s levels due to the induction effect were also observed in a-SiO_x and a-SiN_x (Hasegawa *et al.* 1992). For an O or N atom in the a-SiO_xN_y bonding networks, when the surrounding O concentration

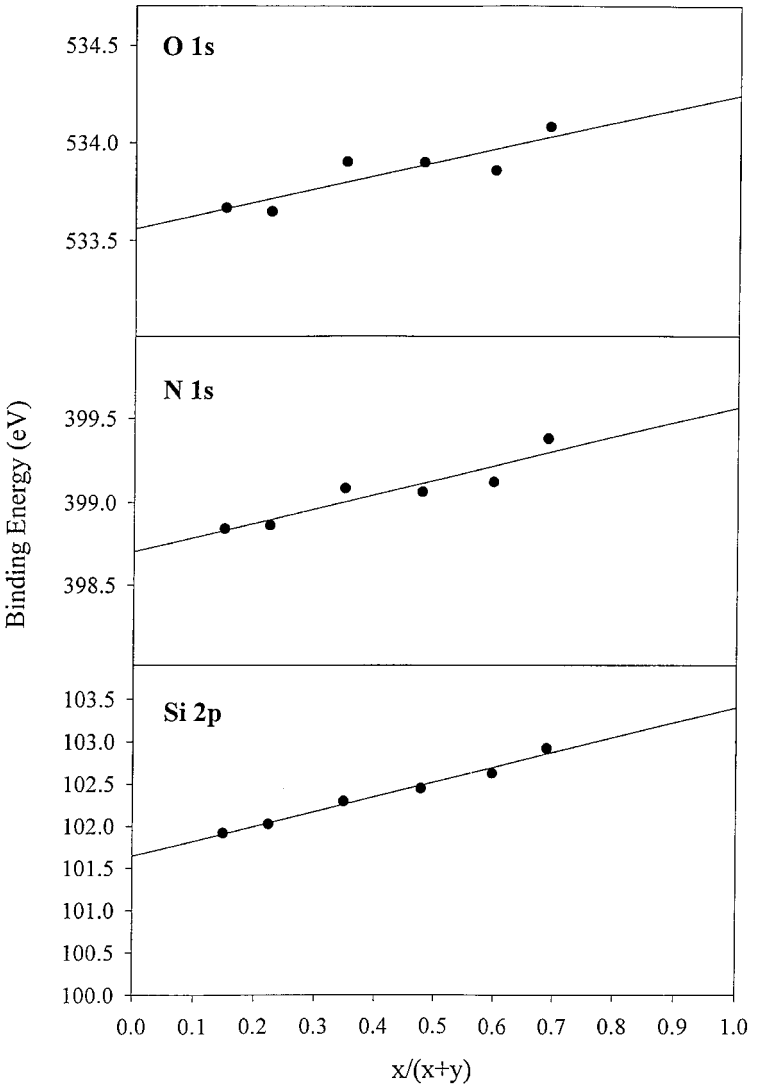

Figure 2. Experimental binding energies of Si 2p, N 1s and O 1s plotted as functions of the composition parameter $x/(x+y)$ for a-SiO_xN_y.

increased, the binding energy of that atom will shift towards a higher energy owing to the deficiency of electron density in the surroundings.

Figure 3 shows the experimental binding energies of the Si 2p, N 1s and O 1s peaks versus the calculated average partial charge at Si, O and N atoms for a-SiO_xN_y with different compositions. The results obtained agree with the conclusion of Pasquarello *et al.* (1995) and Zhang *et al.* (1998) that the second-neighbour effects are important to the binding energy shift.

§4. Cathodoluminescence study

To study the defect properties of short-range order in a-SiO_xN_y, the CL properties of the samples were also investigated. The CL spectra of a-SiO_xN_y films of

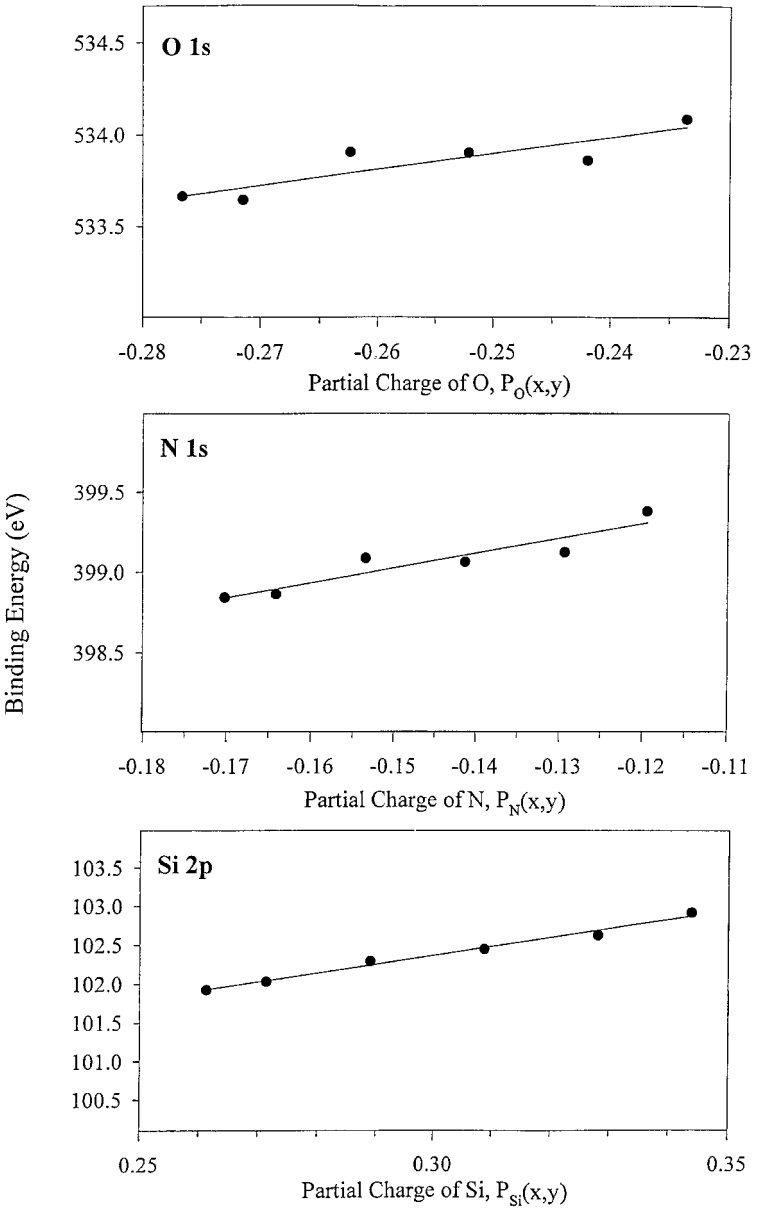

Figure 3. Experimental binding energies of Si 2p, N 1s and O 1s versus average partial charges on the Si, N and O atoms calculated for different compositions of a-SiO$_x$N$_y$ based on the RB model.

different compositions are shown in figures 4 and 5. There are CL bands with energies in the range 1.9, 2.7, 3.1, 3.4–3.6 and 4.4–4.7 eV and a shoulder at an energy of 5.4 eV.

It is well established by electron spin resonance (ESR) and PL that the R centre has an energy of 1.9 eV and a FWHM of 0.2 eV in SiO_2. This centre is due to the O atom with an unpaired electron $\equiv SiO\cdot$ (Skuja 1994a). In the $SiO_{0.95}N_{0.79}$ film, a

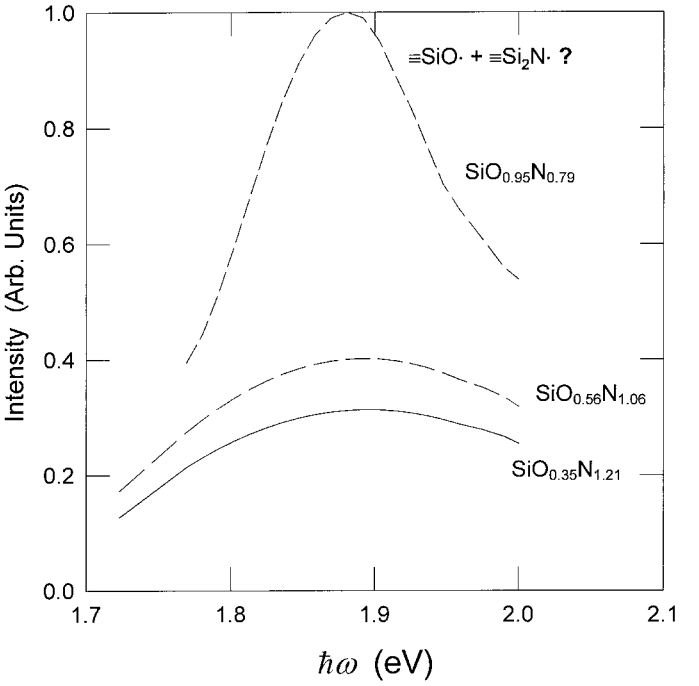

Figure 4. Cl spectra of a-SiO_xN_y in the visible and near-infrared range.

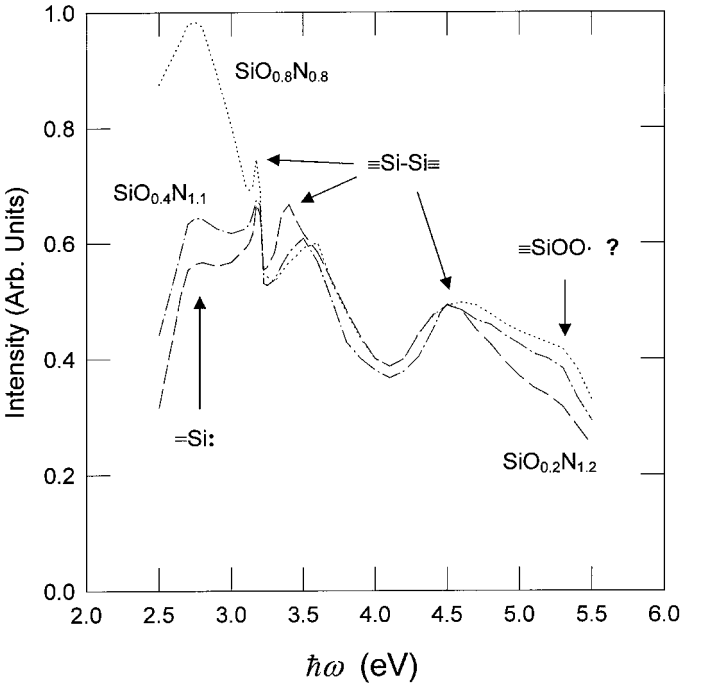

Figure 5. CL spectra of a-SiO_xN_y of different compositions in the visible and near-ultraviolet range. Spectra were normalized with the intensity at an energy of about 4.6 eV.

peak with an energy of 1.9 eV with a FWHM of about 0.2 eV was observed. The intensity of this peak becomes higher as the O concentration in a-SiO_xN_y increases. This observation can be explained as the high density of the $\equiv SiO\cdot$ defect in high-O concentration samples. On the other hand, an increase in the N concentration gives rise to an increase in the FWHM and a shift of the peak to a lower energy (see figure 5).

Analogous to the $\equiv SiO\cdot$ defect in SiO_2, we propose that there exist some $\equiv Si_2N\cdot$ defects in a-SiO_xN_y. This defect was indeed identified by ESR measurement in Si_3N_4 and SiO_xN_y by Warren *et al.* (1990) and Chaiyasena *et al.* (1991) respectively. Since the 1.8 eV CL peak was also found in Si_3N_4 films (Pundur *et al.* 1985, Gritsenko and Pundur 1986), we proposed that the 1.8 eV peak is due to the $\equiv Si_2N\cdot$ defect. Depending on the amount of $\equiv SiO\cdot$ and $\equiv Si_2N\cdot$ defects, the peak position may vary. A low-energy shift can be observed in high-N concentration samples because of the increase in the $\equiv Si_2N\cdot$ defects. It is noted that the Si atoms in the $\equiv SiO\cdot$ and $\equiv Si_2N\cdot$ defects in SiO_xN_y have a more complicated structure than in SiO_2 and Si_3N_4. The Si atoms in these defects can be randomly coordinated by different numbers of O and N atoms. For instance, the $\equiv SiO\cdot$ defect in a-SiO_xN_y may have any kind of configuration given by $O_{3-\beta}N_\beta SiO\cdot$, where $\beta = 0$, 1, 2 and 3. As a result, a slightly different peak energy may be observed.

The blue luminescence band with an energy of 2.7 eV was found in SiO_2 and was attributed to the triplet–singlet transitions in a twofold-coordinated Si atom with two unpaired electrons ($=Si:$) (Skuja 1994a). This peak is also observed in our a-SiO_xN_y samples. The intensity of this peak in a-SiO_xN_y was found to increase when the O concentration increased. We propose that the blue CL peak in SiO_xN_y at 2.7 eV is a result of the sililene centre ($=Si:$) transition. In SiO_2, the Si atom of the sililene centre is coordinated by two O atoms ($O_2Si:$) whereas, in a-SiO_xN_y, the Si atom of the silene centre can be coordinated by two O atoms ($O_2Si:$), by two N atoms ($N_2Si:$), and by one Si atom and one O atom ($NOSi:$). It is not clear whether there exists other kinds of twofold-coordinated sililene defect in addition to the well established $O_2Si:$ defect. Nevertheless, since the intensity of the blue band increases with increase in the O concentration, the $O_2Si:$ defect was definitely present.

The sharp peak with an energy of 3.16 eV and peaks with energy 3.4–3.6 and 4.4–4.7 eV were observed in the CL study of Si_3N_4 films (Pundur *et al.* 1985, Gritsenko and Pundur 1986, Gritsenko 1988, 1993) and were proposed to be governed by the $\equiv Si-Si\equiv$ bonds. The energy of the 3.4–3.6 eV band depends on the Si_3N_4 fabrication method and annealing conditions (Vasilev *et al.* 1986). In Si_3N_4 the intensity of the 4.6 eV peak and the 3.4–3.6 eV band are comparable (Gritsenko 1993). This observation (see figure 4) is evidence for the presence of the $O_2Si:$ centre and $\equiv Si-Si\equiv$ bond. A narrow CL peak with a FWHM of 2.5 nm and an energy of 3.12 eV was also observed in Si_3N_4 films (Pundur *et al.* 1985, Gritsenko and Pundur 1986, Gritsenko 1993). It was proposed that this peak is due to the Si—Si bond, and the narrow width related to the stimulated radiation in Si_3N_4.

The CL band with an energy of 4.4–4.7 eV observed in this work may be interpreted with different defects. The singlet–singlet transition with an energy of 4.4 eV due to the a sililene centre $=Si:$ has been observed in SiO_2 samples (Skuja 1994a). As shown in figure 5, the intensity of the triplet–singlet blue band (2.7 eV) decreases with decrease in the O concentration in SiO_xN_y. However, the ultraviolet band at 4.4–4.7 eV does not have the same trend. Hence the 4.4–4.7 eV band in SiO_xN_y should not be related to the $\equiv Si-Si\equiv$ defect. The 4.4 eV band may be due to the

O_3Si—SiO_3 defect (O vacancy) in SiO_2 as the excitation energy of this band in SiO_2 can be as high as 7.6 eV (Gee and Kastner 1979). In the second case the 4.4–4.7 eV band may be due to the optical transition of the N_3Si—SiN_3 defect in Si_3N_4 samples (Punder *et al.* 1985, Gritsenko 1993). This transition has energy in the same range as the observed CL band. The energy difference between σ-bonding and σ*-antibonding states of the Si—Si bond in Si_3N_4 is 4.6 eV (Gritsenko 1988). It was proposed that the 4.6 eV CL band in Si_3N_4 is related to the antibonding–bonding orbitals of the singlet–singlet transition in the N_3Si—SiN_3 bond without the Stokes shift (Gritsenko 1993).

A shoulder at 5.4 eV was observed in the CL spectra depicted in figure 5. The intensity of this peak increases with increasing O concentration. In SiO_2, an optical absorption at 5.3 ± 0.2 eV has been observed (O'Reilly and Robertson 1983, Bobyshev and Radzig 1988), which is attributed to the peroxy radical $\equiv SiOO\cdot$. Since the energy levels are so close, it is possible that the CL shoulder at 5.4 eV is due to the peroxy radical. The strongly localized wavefunction of unpaired electrons should cause a small electron–phonon coupling and hence results in a small Stokes shift. This is similar to the red 1.9 eV band of the $\equiv SiO\cdot$ defect in SiO_2, which has an excitation energy of 2.0 eV (Griscom 1985, Skuja 1994b).

§ 5. Photoluminescence study

Figure 6 shows the PL excitation with a 5.9 eV source. An asymmetric band at 2.4–3.0 eV was observed. The excitation spectra of this band had a shoulder at 5.7 eV and a maximum at about 6.3 eV. We speculate that the observed PL peaks in figure 3 are related to the Si—Si bond in a-SiO_xN_y. Performing numerical simulation using MINDO/3, we found that the Si—Si bond in silicon nitride can capture both an electron and a hole (Gritsenko *et al.* 1998a). The energy level of the bonding orbital for the Si—Si bond is close to the top energy of the valence band (−2.0 eV) and the antibonding orbital level is located near the bottom of the conduction band (−6.5 eV) (Gritsenko *et al.* 1998a). These results support the speculation that we have made. However, more experiments should be conducted to confirm this conjecture further. It is also noted that the PL spectra show a large Stokes shift (Gee and Kastner 1979), which is evidence of very strong electron–phonon coupling in a-SiO_xN_y.

§ 6. Concluding remarks

In conclusion, we found that the short-range order of a-SiO_xN_y can be quantitatively described by the RB model. According to this model, a-SiO_xN_y consists of bonded networks composed of five sorts of randomly distributed tetrahedra: $SiO_\nu N_{4-\nu}$ ($\nu = 0$, 1, 2, 3 and 4). Since a-SiO_xN_y is not a mixture of a-SiO_2 and a-Si_3N_4 clusters, the gate oxynitride in MOS device does not have gigantic surface potential fluctuations in the vicinity of the channel resulting from the spatial local fluctuations in the dielectric permittivity. In addition, we found that the chemical shifts of the Si 2p, N 1s and O 1s levels depend not only on the nearest neighbours but also on the second- and even further-neighbour atoms.

The validity of the Mott rule for SiO_xN_y opens up the possibility for proposing a more specific definition for point defects in an amorphous solid. According to Elliott (1994), a *point defect* is any deviation from the coordination number described by the Mott rule and from the expected sorts of atoms in the formation of the bonds with

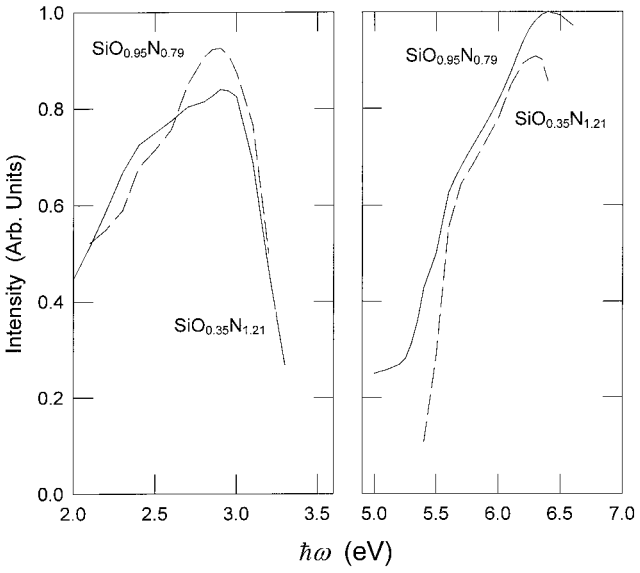

Figure 6. PL spectra of a-SiO$_x$N$_y$ in the visible and ultraviolet range: (*a*) luminescence at an excitation energy of 5.9 eV; (*b*) excitation spectra of the PL band with an energy of 2.7 eV.

respect to an 'ideal' (defect-free) structure. In SiO_2 and Si_3N_4, the defects associated with this definition include the following:

(*a*) paramagnetic defects such as ≡Si·, ≡Si—O—O· and ≡Si$_2$N·;
(*b*) diamagnetic defects such as ≡Si—Si≡, =N—H and the sililene centre =Si:;
(*c*) neutral defects such as ≡SiO·, =Si:, ≡SiOH, ≡Si—O—O—Si≡;
(*d*) charged defects such as ≡Si· $^{+}$Si≡ (E′ centre in SiO_2) (Rudra and Fowler 1987) and ≡Si$_2$N: (electron captured by the ≡Si$_2$N· defect in oxynitride);
(*e*) intrinsic defects such as ≡Si·, =N—N=, ≡Si—O—O—Si≡ and =Si:;
(*f*) extrinsic defects such as ≡SiH, ≡Si$_2$NH and ≡SiOH.

The RB model and Mott rule together explained the trap centre and the process-dependent trapping characteristics of the oxynitride and the oxide–nitride interface observed previously (Gritsenko *et al.* 1999). For the CL and PL studies, a CL band at 1.8–1.9 eV is observed and is attributed to the —SiO· and ≡Si$_2$N· defects. Peaks at 3.16, 3.4–3.6 and 4.4–4.7 eV were attributed to the N_3Si—SiN_3 bonds. The peak at 5.4 eV was attributed to the peroxy radical. However, it is still unclear why the 2.3–2.4 eV level, which is typical for a PL centre in Si_3N_4 (Vasilev *et al.* 1986, Seol *et al.* 1999), is not found in oxynitride.

References

Bosyshev, A. A., and Radzig, V. A., 1988, *Phys. Chem. Glasses,* **14**, 501.
Britov, I. A., Gritsenko, V A., and Romaschenko, Yu. N., 1985, *Soviet. Phys. JETP,* **62**, 321.
Chaiyasena, I. A., Lenahan, P. M., and Dunn, G J., 1991, *Appl. Phys. Lett.,* **58**, 2141.

ELLIOTT, S. R., 1994, *Defects and Disorder in Crystalline and Amorphous Solids,* NATO Advanced Study Institute Series, Series C, Vol. 418, edited by C. R. A. Catlow (Boston, Massachusetts: Kluwer), pp. 73–86.
GEE, C. M., and KASTNER, M., 1979, *Phys. Rev. Lett.,* **42**, 1765.
GRISCOM, D. L., 1985, *J. non-crystalline Solids,* **73**, 51.
GRITSENKO, V. A., 1988, *Silicon Nitride in Electronics* (New York: Elsevier); 1993, *Structure and Electronic Properties of Amorphous Dielectrics in Silicon MIS Structures* (Novosibirsk: Science), p. 280.
GRITSENKO, V. A., KOSTIKOV, YU. P., and ROMANOV, N. A., 1981, *JETP Lett.,* **34**, 3.
GRITSENKO, V. A., NOVIKOV, YU. N., MOROKOV, YU, N., and WONG, H., 1998a, *Microelectron Reliability,* **38**, 1457.
GRITSENKO, V. A., and PUNDUR, P. A., 1986, *Soviet Phys. Solid St.,* **28**, 1829.
GRITSENKO, V. A., SVITASHEVA, S. N., PETRENKO, I. P., WONG, H., XU, J. B., and WILSON, I. H., 1999, *J. electrochem. Soc.,* **146**, 780.
GRITSENKO, V. A., XU, J. B., KWOK, R. W. M., NG, Y. H., and WILSON, I. H., 1998b, *Phys. Rev. Lett.,* **81**, 1054.
HASEGAWA, S., HE, L., INOKUMA, T., and KURATA, Y., 1992, *Phys. Rev.* B, **46**, 12 478.
KARCHER, R., LEY, L., and JOHNSON, R. L., 1984, *Phys. Rev.* B, **30**, 1896.
KUBLER, L., HAUG, R., RINGEISEN F., and JAEGLE, A., 1983, *J. non-crystalline Solids,* **54**, 23.
LU, H. C., GUSEV, E. P., GUSTAFSSON, T., GARFUNKEL, E., GREEN, M. L., BRASEN, D., and FELDMAN, L. C., 1996, *Appl. Phys. Lett.,* **69**, 2713.
O'REILLY, E. P., and ROBERTSON, J., 1983, *Phys. Rev.* B, **27**, 3780.
PASQUARELLO, A., HYBERTSEN, M. S., and CAR, R., 1995, *Phys. Rev. Lett.,* **74**, 1024.
PAULING, L., 1960, *The Nature of Chemical Bonds,* third edition (Ithaca, New York: Cornell University Press), p. 85.
PHILIPP, H. R., 1972, *J. non-Crystalline Solids,* **8–10**, 627.
PUNDUR, P. A., SHAVALGIN, YU. G., and GRITSENKO, V. A., 1985, *Phys. Stat. sol.* (a), **94**, K107.
RAIDER, S. I., FLITSH, R., ABOAF, J. A., and PLISKIN, W. A., 1976, *J. electrochem. Soc.,* **123**, 560.
ROBERTSON, J., 1994, *Phil. Mag.* B, **69**, 307.
RUDRA, J. K., and FOWLER, W. B., 1987, *Phys. Rev.* B, **35**, 8223.
SEOL, K. S., FUTAMI, T. F., WATANABE, T., and OHKI, Y., 1999, *J. appl. Phys.,* **85**, 6746.
SKUJA, L., 1994a, *J. non-crystalline Solids,* **167**, 229; 1994b, *ibid.,* **179**, 51.
VASLIEV, V. V., MIKHAILOVSKII, I. P., and SVITASHEV, K. K., 1986, *Phys. Stat. sol.* (a), **95**, K37.
WARREN, W. L., LENAHAN, P. M., and CURRY, S. E., 1990, *Phys. Rev. Lett.,* **65**, 207.
ZHANG, K. Z., LITZ, K. E., and HOLL, M. M. B., 1998, *Appl. Phys. Lett.,* **72**, 46.